Modeling, Simulation and Validation of the Mo and Mo^+ Deposition Imparted by the NASA Evolutionary Xenon Thruster (NEXT)

IEPC-2017-281

Presented at the 35th International Electric Propulsion Conference
Georgia Institute of Technology – Atlanta, Georgia – USA
October 8–12, 2017

Luis M. Bermúdez* and Joel B. Jermakian†
Space Systems Group, Orbital ATK, Inc., Dulles, VA 20166-6874, USA

Over the last few years the Space Systems Group of Orbital ATK has been working towards the technology infusion of Electric Propulsion (EP) in all aspects of the engineering design, manufacturing processes and mission operations with significant effort being dedicated to the EP system integration, and its impact on other subsystems and the overall spacecraft performance. In particular, operation of the NASA Evolutionary Xenon Thruster (NEXT) causes sputtering of material eroded from the extraction grids that can get ionized after interacting with the plasma plume and contaminate sensitive parts of the spacecraft following the plasma plume induced electrical field. Within this scope, the paper hereafter reports the work performed to develop a validated NEXT simulation model within the COLISEUM framework that is capable of modeling the entire spacecraft while achieving a desired balance between fidelity and runtime. Validation against experimental data is presented along with a sensitivity study to improve agreement between simulations and experiments for anomalously high erosion at specific thrust levels (TLs). Potential future model improvements and further studies are also suggested.

Nomenclature

e	Elementary charge, C
J^+	Xe single ion total current, A
J^{++}	Xe double ion total current, A
k_B	Boltzmann constant, J/K
n_e	Plasma number density, $\#/m^3$
T_e	Plasma temperature, eV
γ	Specific heat ratio
ϕ	Plasma potential, V
Superscripts	
*	Reference value

*Staff Systems Engr., Systems Engineering Dept.
†Senior Staff Systems Engr., Systems Engineering Dept.

I. Introduction

The last decade has seen an increase in the activities directed at the understanding and modeling of the flow physics generated in EP devices. The surge in interest has been mainly motivated by the adoption of EP thrusters as a technically viable and more mass efficient solution for spacecraft propulsion and by the need to understand the spacecraft interaction with the plume generated by these devices. On one side, NASA, DoD, and other research organizations have been at the forefront of the R&D effort conducting first-of-a-kind tests to uncover new physics, formulating mathematical models that allow further understanding, and advancing the simulation techniques which together have provided higher fidelity and more capable tools for the study and characterization of EP thruster flows and plumes. On the other side, industry leaders such as Orbital ATK have adopted these tools in analytical processes, augmenting existing capabilities in some instances, and contributing to the EP technology maturation roadmap.

Since 2013 the Space Systems Group of Orbital ATK has been working towards the technology infusion of EP in all aspects of the engineering design, manufacturing processes and mission operations of its Commercial, Science & Environmental, National Security, and Human Space & Advanced Systems spacecraft product lines. To this end, the GEOStar-3 bus offers now the replacement of heritage Improved Electrothermal Hydrazine Thrusters (ImpEHTs) by the XR-5 Hall Effect Thruster (HET). The Mission Extension Vehicle (MEV) which will provide cooperative in-orbit satellite life extension and maneuvering services to geosynchronous satellite operators will also incorporate HETs for orbit raising, station keeping and inclination reduction. In addition to these, several other spacecraft currently in the proposal and design stages will incorporate different types of EP solutions, including NEXT and others.

With the adoption of any new technology there are also challenges that must be overcome. For a spacecraft manufacturer these challenges are very often associated with the EP system integration and its impact on other subsystems and the overall spacecraft performance. In particular, a new area of concern is the one represented by the plasma plume interaction effects on the spacecraft. These interaction include physical (i.e. erosion, sputtering and contamination), mechanical (i.e., induced forces and moments), electrical (i.e. spacecraft charging), and electromagnetic (i.e. telecommunications interference) effects. Before a spacecraft design can be frozen for production, its performance characteristics must be correctly assessed including all the nuances introduced by the inclusion of a new EP platform.

With respect to the NEXT, operation of this ion engine causes the sputtering of material eroded on the extraction grids, mainly from impingement by ions formed by charge exchange collisions (CEX). Even though the sputter rate is low, the primary failure mechanism of the NEXT is expected to result from degradation of the acceleration grid structure by this action.[1] Furthermore, this sputtering phenomenon has the potential for detrimental effects from a spacecraft/engine integration point of view. The deposition of the Mo particle flux emanating from the NEXT extraction grids and the subsequent generation of Mo ions by CEX between the sputtered material and the Xe ions could negatively affect the spacecraft surface properties. It is this potential for deposition on spacecraft surfaces which is the focus of this paper.

The aforementioned deposition of Mo neutrals and ions on the spacecraft surfaces requires a thorough assessment during the design phase. The objective is to deliver a robust design where the spacecraft performance is not compromised in any manner by the use of NEXT during its projected life. The modeling and simulation (M&S) required for such assessment carries the challenge of including sufficient fidelity in the predictions for a multiscale/multiphysics problem which is intractable for first-principles numerical simulation. In the work presented hereafter this challenge is met by using AFRL's COLISEUM framework with series of empiricisms based on observations published for the NEXT during the last decade. An attempt is also made to validate this approach and provide a quantifiable level of uncertainty.

II. Modeling & Simulation

Deposition of Mo neutrals and ions on the spacecraft surfaces resulting from the use of NEXT was analyzed building on the work published by Brieda *et al.* in Ref. 2. However, rather than being concerned with the electron dynamics in the plume and the beam neutralization process, the analysis presented hereafter focuses on the particle collision dynamics and surface-particle interactions as a way to address the effect of the Mo contamination on the spacecraft surface properties. To this end the analysis makes use of two of the modules included in AFRL's COLISEUM framework: Volcar, which is the mesh generator with support for particle-surface interaction, and Draco, which is the finite-difference structured grid electrostatic

(ES) particle-in-cell (PIC) with support for particle-particle interactions. The analysis relaxes some of the constraints of the original work while imposing other assumptions to achieve the desired balance between fidelity and simulation runtime. The goal is that while these simplifying assumptions will allow for a complete system analysis, they do not invalidate this approach and make the solution impractical.

The simulation process starts with a discretized representation of the configuration surface as shown in Fig. 1 for the NEXT in this case. Surfaces are represented in COLISEUM as collections of triangles (elements) grouped into components. The discretized geometry is embedded in a cartesian background grid which defines the computational domain for the PIC simulation. Species macroparticles (e.g. simulated particles consisting of a number of physical particles) are injected into the simulation by specifying fluxes from surface elements (e.g. acceleration grid and neutralizer) following distribution functions that are adjusted based on the nature of the particle (e.g. Xe ions, Xe neutrals or Mo neutrals).

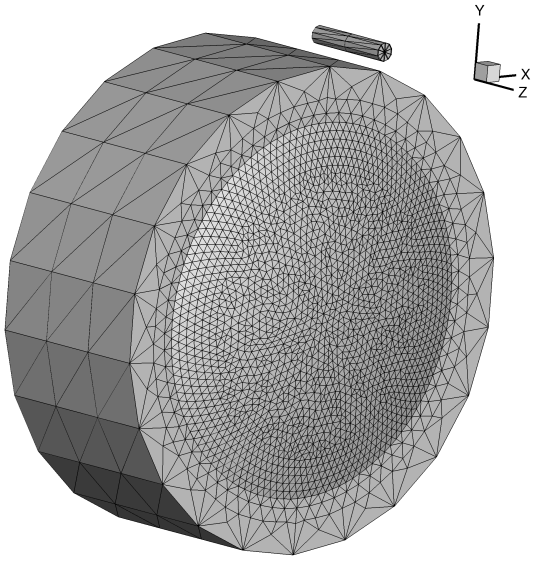

Figure 1. Surface discretization of NEXT.

Unlike in the original work where the plasma plume accounted for Xe single charged ions and electrons, the model described in this paper includes Xe neutrals as well as single and double charged ions. It was found that these new plume constituents play a significant role in defining the plume characteristics through the collisions dynamics implemented.

Particle injection of the Xe neutrals and Xe ions from the acceleration grid follows a shifted Maxwell-Boltzmann distribution with the radial flux adjusted according to a given profile (see Fig. 2) based on experimental current density distributions reported in Ref. 3. Also, in this model, the neutralizer serves only as a source of Xe neutrals. Xe neutrals are injected in this case following a shifted Maxwell-Boltzmann distribution. The required Xe neutral and ion mass flow rates, and charge ratio (J^{++}/J^{+}) are taken from Refs. 4 and 5 for each of the TLs in throttle table 11 (TT11) which was developed for planetary science missions. In addition, ion and neutral velocities are calculated using the beam voltage for each of the TLs and estimated following eq. 1 in Ref. 6, respectively. Finally, the temperature of the emitted material is assumed to be equal to the wall temperatures which are also taken from Ref. 6.

An ion optics code is not used to calculate the angular distribution of current in the beamlet (i.e. current through a single hole in the acceleration grid). On the contrary a fully kinetic approach is used where particles are introduced relative to the normal vector of the source triangle, hence, resulting in approx. 16 deg beam divergence due to the physical curvature of the surface mesh. This characteristic of the particle injection model in COLISEUM is modified to account for the divergence half-angle at 95% of beam current reported in Ref. 7.

Because of limitations imposed by the COLISEUM particle injection library, Mo neutrals are injected following a zero-shift Maxwell-Boltzmann distribution with a temperature selection corresponding to half the Mo binding energy rather than using a Sigmund-Thompson distribution.[8] As Fig. 3 depicts, this results

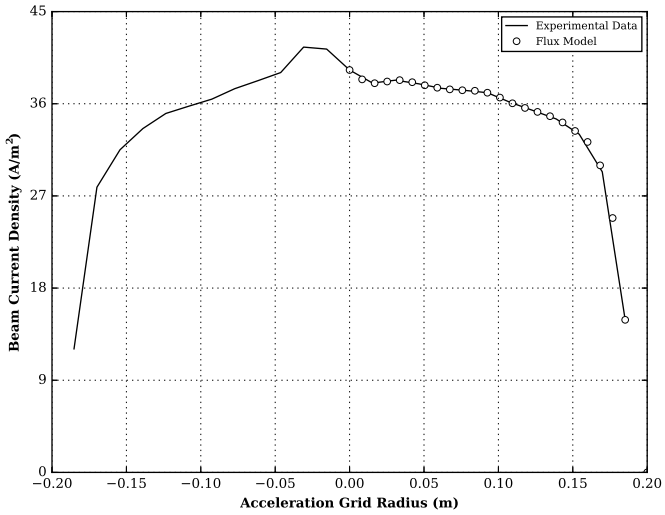

Figure 2. Beam current density versus radial distance at 3 cm for TL37.

in a higher number of Mo neutrals introduced at lower speeds but with the exact same "most probable speed". The acceleration grid wear in the bulk of the throttle conditions is dominated by the erosion of the downstream side of the accelerator electrode due to charge-exchange ion impingement. For the purpose of this effort, the Mo mass flow rate needed by the particle injection algorithm is taken from the estimated acceleration grid mass loss rate in Ref. 1 using the computation where variable Mo weight fraction is assumed. In that case, the Mo abundance is proportional to the sum of Mo, C, and O abundance, and a Mo cosine distribution from high angles up to the thrust axis is assumed.

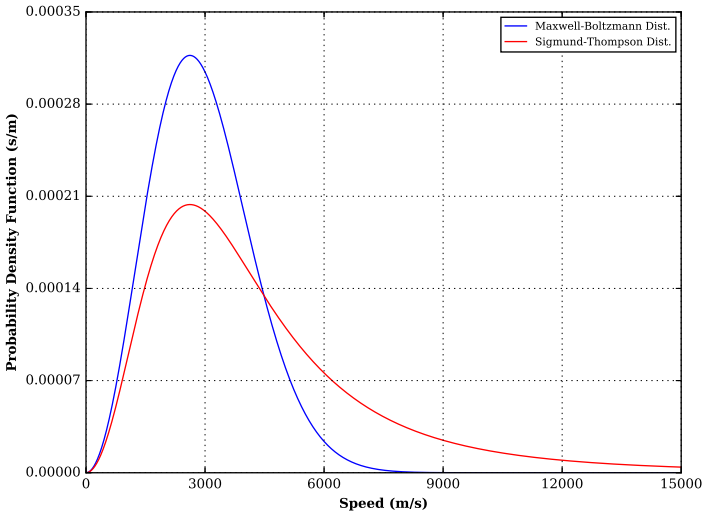

Figure 3. Maxwell-Boltzmann vs. Sigmund-Thompson velocity distributions.

As part of the collision dynamics, it is estimated that a small fraction of sputtered Mo atoms are ionized by Xe single charged ions accordingly to:

$$\mathrm{Xe}^{+1} + \mathrm{Mo} \longrightarrow \mathrm{Xe} + \mathrm{Mo}^{+1} \tag{1}$$

The CEX cross sections between Xe ions and Mo neutrals are approached by a logarithmic model based

on the experimental data published in Ref. 9 and depicted in Fig. 4. However, the population of Mo ions is expected to be underestimated based on the fact that, as it was mentioned before, Mo atoms are injected at lower speeds than it is realistic. This results in the speed relative to the Xe ions being higher and therefore less likely to collide. This deficiency in the Mo ion population is difficult to assess since there is no experimental data reporting, directly or indirectly, the amount of this constituent in the plume.

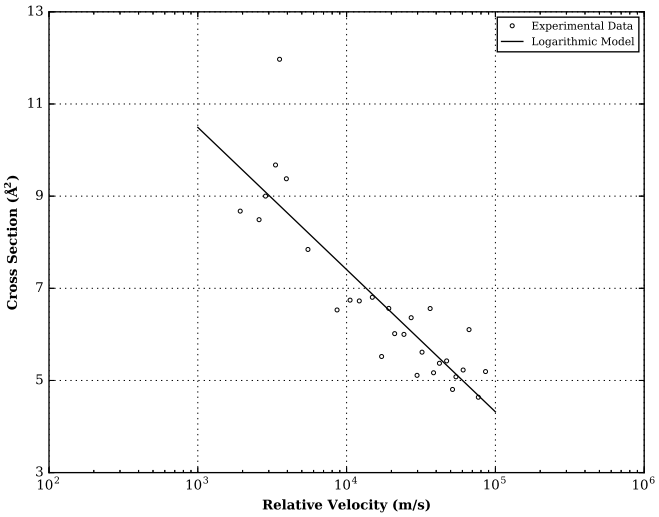

Figure 4. CEX cross sections between Xe^{+} and Mo.

In addition to this, two more CEX collision events between Xe ions and neutrals are modeled in COLISEUM following the implementation based on differential cross sections described by Scharfe *et al.* in Ref. 10. In these two events, Xe single charge and double charge ions are formed by the following CEX symmetric reactions:

$$Xe^{+1} + Xe \longrightarrow Xe + Xe^{+1} \tag{2}$$

$$Xe^{+2} + Xe \longrightarrow Xe + Xe^{+2} \tag{3}$$

Cross sections are taken from Ref. 11 which are logarithmic fits to experimental data. The energy values of the Xe ions in the plume that go through the CEX collision dynamics aforementioned exceed the range of energies for which these cross section models are derived. Regardless of this shortcoming, these models are maintained and used in the simulation.

All the CEX processes described above are treated in COLISEUM using a rudimentary Monte Carlo Collision (MCC) method. The MCC method performs collisions by colliding particles with a background target "cloud". Unlike the Direct Simulation Monte Carlo (DSMC) method, the MCC method does not require sampling of two particles from the same cell which improves the simulation runtime. However, since only one particle is involved in an MCC collision, mass and momentum are not conserved. MCC instead assumes that the background cloud is very massive such that it is not affected by collisions.[12] This assumption is corroborated by the discrepancy in size between the target and product populations present in each one of the simulations carried out in this work using the MCC method.

Finally and with respect to the potential field calculation, rather than solving the Poisson equation, it is defined using the polytropic Boltzmann relationship:

$$\phi - \phi^* = \frac{k_B T_e^*}{e} \frac{\gamma}{\gamma - 1} \left[\left(\frac{n_e}{n_e^*} \right)^{\gamma - 1} - 1 \right] \tag{4}$$

where the reference plasma temperature (T_e^*), reference plasma potential (ϕ^*) and the reference plasma density (n_e^*) require previous knowledge of the plasma plume and are, therefore, taken from Ref. 13 for TL40 and estimated for all other TLs due to the lack of experimental data. When estimated, the reference plasma temperature is kept constant while the reference density is scaled using the beam current and the reference plasma potential is set using the same correlation as reported in Fig. 7 of Ref. 14.

III. Validation

With all the model inputs in place, a series of simulation test cases were conducted with the objective of assessing the model validity. The first of these tests measured the energy content in a particular location in the plume and compared it against experimental data. Off-axis retarding potential analyzer (RPA) data was collected and reported in Ref. 15 for three operating conditions similar to TL5, TL19, and TL40. This data shows that not only the most probable ion energy matched the beam voltage but also that high-energy ions are present at 45 deg off the thruster axis at all operating conditions. This important plume-spacecraft interaction aspect, as pointed out in Ref. 15, is reproduced in the NEXT simulations for TL5, TL19, and TL40 using the background pressure reported for this particular test and the model inputs described before (see Fig. 5).

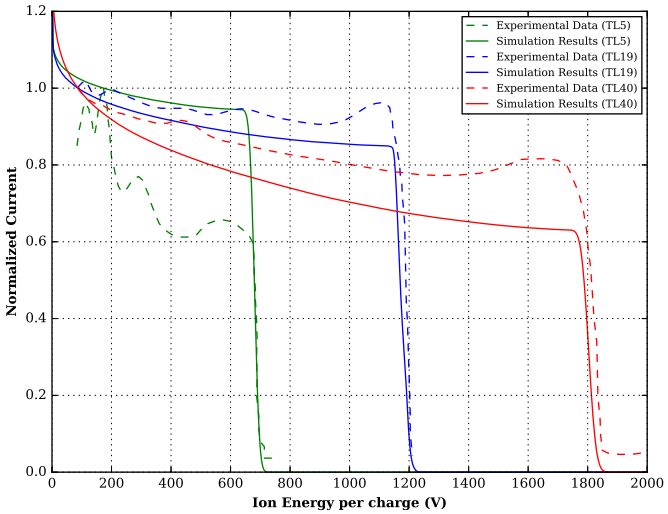

Figure 5. RPA data at 1 m distance and 45 deg plume angle for TL5, TL19 and TL40.

The information presented in Fig. 5 also shows how there is a small population of ions at other energies than at the beam voltage. Those ions are produced by collisions. The numerical results do not accurately reproduce these populations. In the case of the medium and high beam current and potential (i.e. TL19 and TL40), the numerical simulation predicts a higher number of low energy ions than what the experimental data shows. This result is reversed for the low beam current and potential case (i.e. TL5) where the experimental data indicates a higher population of the low energy ions.

The next step in the validation process utilized field data from plume characterization tests reported in Ref. 3 in which experimental measurements were performed using an engineering model thruster (i.e. EM4) having a 36-cm ion optics. Simulations mimicking the test setup and conditions were carried out. Comparisons between the experimental and numerical plasma potential contours are presented in Fig. 6. The most noticeable difference in those contours occurs predominantly outside of the main beam. The fidelity of the plasma plume in that area, in particular, is expected to be the most impacted by the effect of the simulated particle collision dynamics. Still the experimental data and simulation results differ less than 1 V in all cases.

The last step in the validation process involved comparing grid material deposition rates between the simulation results and the experimental data for two of the thrust levels reported in Ref. 1. During this test a rotatable quartz crystal microbalance (QCM) recorded the rate of Mo deposition at 1-m distance for a range of plume angles between 58 and 90 deg in 4-deg increments. Fig. 7 shows the test set up used in the QCM measurements and the simulated Mo plume ejected from the acceleration grid.

NEXT incorporates two extraction grids: a screen grid and an acceleration grid. As mentioned before, Mo erosion occurs primarily on the acceleration grid mainly from CEX ion impingement. Net deposition rates measured by the QCM during this test are the result of two competing effects: mass arrival rate of retained Mo and residual gases, and mass removal rate by incoming energetic plume ions. Residual gases

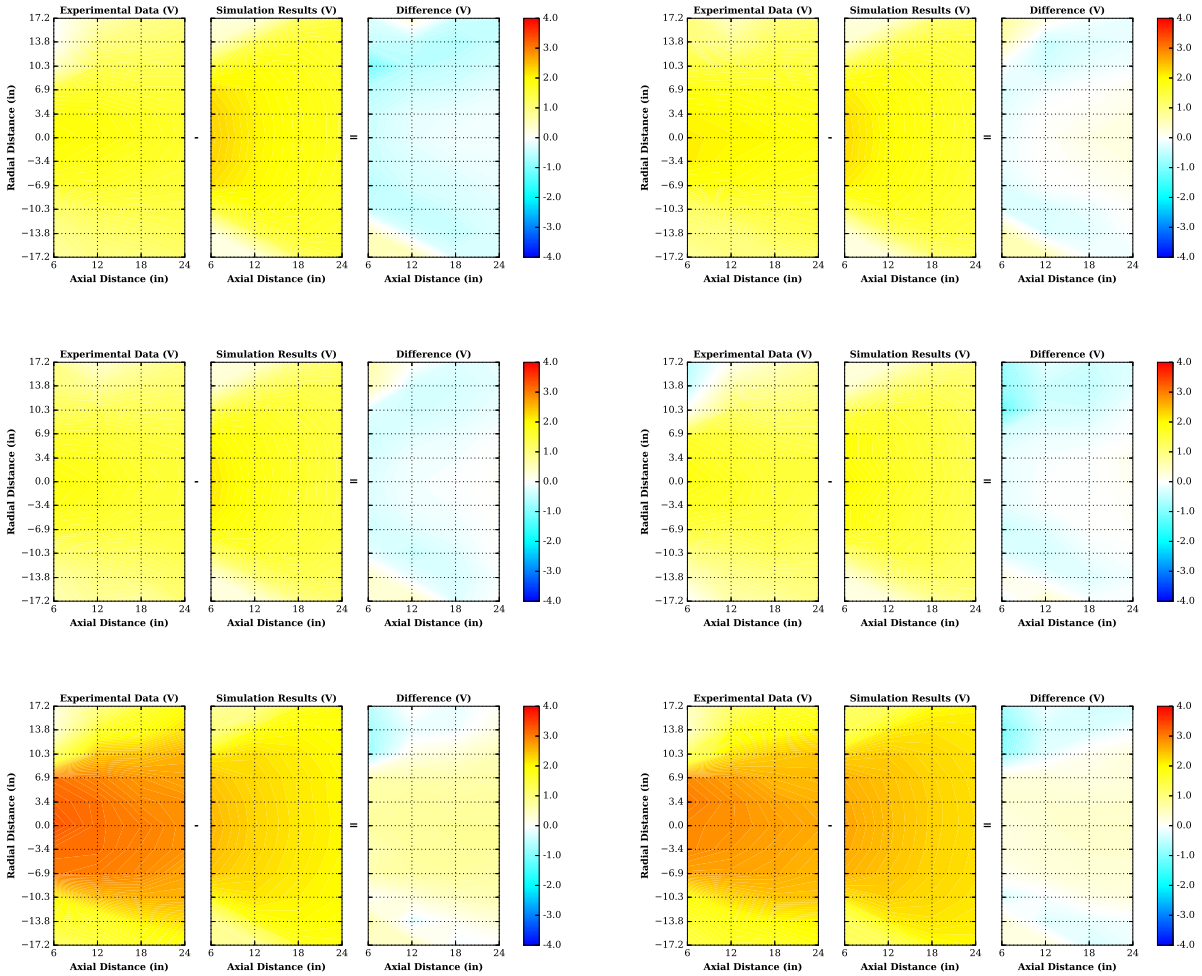

Figure 6. Plasma potential comparisons for TL1, TL5, TL9, TL12, TL19 and TL37 (thrust level contours are organized form left to right and top to bottom, respectively).

in the test chamber react with deposited Mo increasing the effective rate of mass influx and modifying the sputter yield of the deposited layer. The Mo arrival rate for this test was estimated after correcting for the weight accumulation of the non-Mo species by means of X-ray photoelectron spectroscopy (XPS) analysis.

Fig. 8 depicts the net mass deposition rate for TL37. The agreement between the experimental data and simulation results is good for high plume angles where the CEX ion population is predominant. However, the comparison worsens near the beam centerline where the more energetic ions reside and the plume structure suffers the most based on the simulation approach taken in this analysis.

As reported in Ref. 1, typical TL12 deposition rate is the highest found despite the low beam current. That is said to be expected since the low beam current and high beam voltage is associated with an under-perveance condition that causes beamlet defocusing and enhances grid erosion. In the current validation study, the mass deposition rate is greatly overestimated for this TL condition, as shown in Fig. 9.

To assess the overestimation of the TL12 net mass deposition, the simulation was executed a second time splitting the Mo mass flow rate equally between two different particle injection algorithms. The first one having the same zero-shift Maxwell-Boltzmann distribution as before while the second one made use of the algorithm described previously for injecting the Xe ions. The concept behind this split is to capture the effects of the different Mo plume particles. The first created by erosion of the downstream side of the accelerator electrode, due to CEX ion impingement, and the second created by the beamlet defocusing phenomenon previously referenced, which is expected to have a plume shape more consistent with the plasma one. Fig. 10 shows the new comparison which corroborates the different nature of the Mo mass deposition.

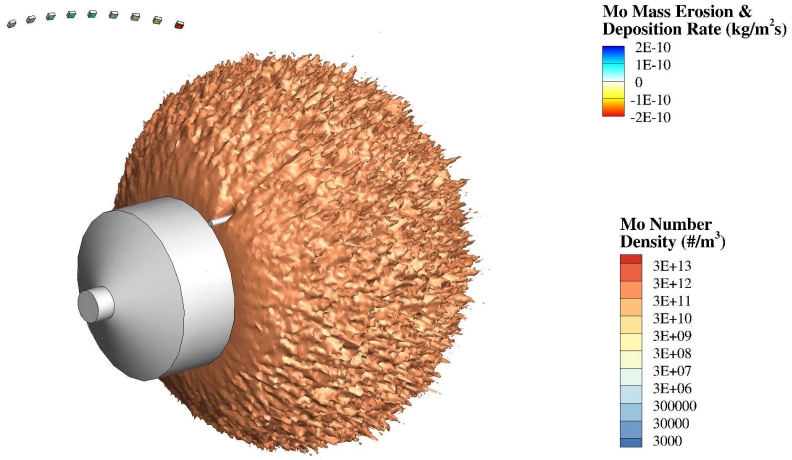

Figure 7. QCM test setup.

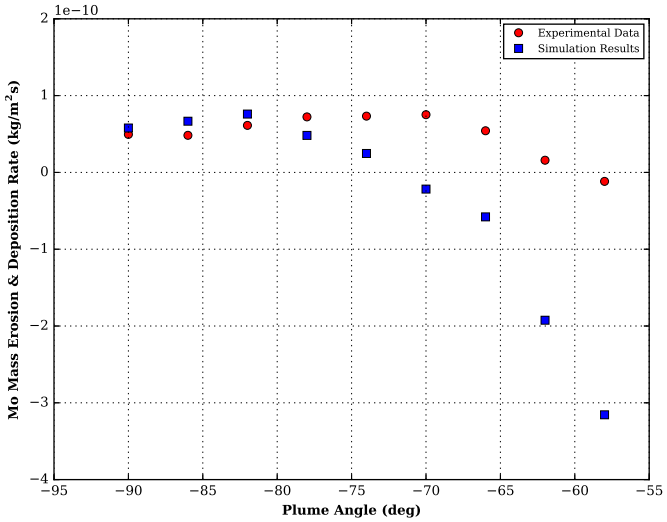

Figure 8. Net mass deposition rate for TL37.

IV. Conclusion

The COLISEUM framework has been shown to be a useful tool in understanding plume effects on spacecrafts due to EP systems. Previous work largely focuses on the direct impact of the plasma plume, notably from Hall Effect Thrusters (HETs) which have a relatively high divergence angle. In this effort, COLISEUM has been used to examine the potential for contamination on spacecraft surfaces of systems incorporating NEXT. Although somewhat empirically based, the use of a zero-shift Maxwell-Boltzmann distribution for the Mo inflow provides good agreement for "well behaved" throttle levels. A hybrid input model using a combination of shifted and unshifted Maxwell-Boltzmann distributions can be used for a better fit of throttle levels where defocused effects cause sputtering from both extraction grids. It should be noted that the work performed shows that agreement between experimental data and simulation results does not necessarily indicate strong agreement between actual use in space and simulation due to chamber

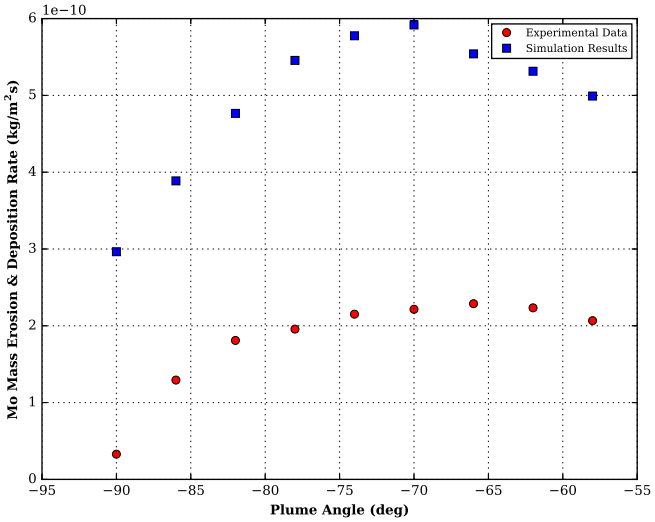

Figure 9. Net mass deposition rate for TL12.

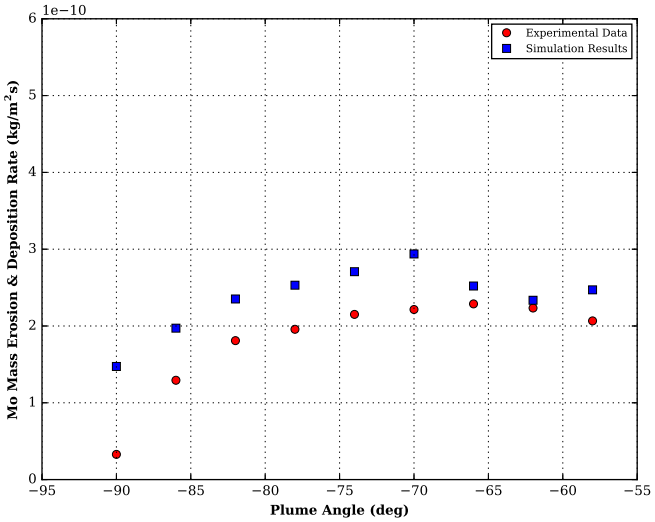

Figure 10. Net mass deposition rate for TL12 after splitting the Mo mass flow rate between two different particle injection algorithms.

effects. However, this is likely to be less impactful at the large angular values which represent the greatest contamination risk.

With respect to the multiple Mo plume injection models used, if one attributes the two injection causes to the two injection models, a further refinement could be incorporated to apportion the relative contributions at each throttle level. This should be done with care unless additional test data, at more throttle levels at which the defocusing effects associated with TL12 are seen. As this is expected behavior, this additional test data can be used with analytical modeling to provide the appropriate function to use for such an apportionment.

Sensitivities to the refinement of the cartesian background grid and the surface mesh were also carried out as part of this work, with results being reported for a discretization level where changes are negligible. In addition to this discretization sensitivity, use of different CEX collision dynamics models within COLISEUM

where tested. It was found during the validation process that the implementation based on differential cross sections was superior in this regard. Lastly, sensitivity studies were also performed using different macroparticle sizes, temperatures of the emitted materials and the reference quantities required to define the potential field. The final macroparticle sizes were chosen to provide consistent collision dynamics within the accuracy of the model while the temperatures of the emitted materials and reference quantities for the potential field were found to have a noticeable effect on the simulation results.

In summary, the approach taken in this work has been to develop the best validated plasma plume model possible and to incorporate a kinetic description of the Mo injection. While this seems to be a good approach for most of the TLs where the Mo sputtering occurs due to CEX ion impingement, it is found that this kinetic description is critical when getting high mass deposition rates. Therefore, a logical next step would be replacing this approach with a beamlet code, which improves the plasma plume representation and the estimate of fast/slow Mo being sputtered from the thruster.

Finally, the work presented here provides a foundation for spacecraft level modeling of deep space missions using NEXT. As a result of such work, Orbital ATK has found integration of NEXT into such missions manageable as long as proper accommodation and mitigation effects are incorporated into the design process.

Acknowledgments

The authors would like to thank Mr. Michael J. Patterson at NASA Glenn Research Center and to Mr. Mark W. Crofton at The Aerospace Corp. for their help interpreting the experimental data collection and reduction.

References

[1]Crofton, M. W., Nocerino, J. C., Young, J. A., and Patterson, M. J., "NEXT Ion Engine Plume Deposition Rates: QCM Measurements," AIAA Paper 2014-0140, *52nd Aerospace Sciences Meeting*, AIAA SciTech Forum, National Harbor, MD, January 2014.

[2]Brieda, L. and Wang, J., "Modeling of Ion Thruster Beam Neutralization Using a Fully Kinetic ES-PIC Code," AIAA Paper 2005-4045, *41st AIAA/ASME/SAE/ASEE Joint Propulsion Conference & Exhibit*, Tucson, AZ, July 2005.

[3]Pollard, J. E., Diamant, K. D., Crofton, M. W., Patterson, M. J., and Soulas, G. C., "Spatially-Resolved Beam Current and Charge-State Distributions for the NEXT Ion Engine," AIAA Paper 2010-6779, *46th AIAA/ASME/SAE/ASEE Joint Propulsion Conference & Exhibit*, Nashville, TN, July 2010.

[4]Van Noord, J. L., Soulas, G. C., and Sovey, J. S., "NASAs Evolutionary Xenon Thruster (NEXT) Prototype Model 1R (PM1R) Ion Thruster and Propellant Management System Wear Test Results," IEPC Paper 2009-163, *31st International Electric Propulsion Conference*, Ann Arbor, MI, September 2009.

[5]Young, J. A., Crofton, M. W., and Diamant, K. D., "Plume Characterization of the NEXT Thruster Under Extended Throttle Conditions," AIAA Paper 2013-4111, *49th AIAA/ASME/SAE/ASEE Joint Propulsion Conference & Exhibit*, San Jose, CA, July 2013.

[6]Van Noord, J. L., "NEXT Ion Thruster Thermal Model," AIAA Paper 2007-5217, *43rd AIAA/ASME/SAE/ASEE Joint Propulsion Conference & Exhibit*, Cincinnati, OH, July 2007.

[7]Soulas, G. C., Haag, T. W., and Patterson, M. J., "Performance Evaluation of 40 cm Ion Optics for the NEXT Ion Engine," AIAA Paper 2002-3834, *38th AIAA/ASME/SAE/ASEE Joint Propulsion Conference & Exhibit*, Indianapolis, IN, July 2002.

[8]Thompson, M. W., "The Energy Spectrum of Ejected Atoms During the High Energy Sputtering of Gold," *Philosophical Magazine*, Vol. 18, No. 152, 1968, pp. 377–414.

[9]Vroom, D. A. and Rutherford, J. A., "Cross Sections for Charge Transfer Between Mercury Ions and Other Metals," NASA CR-135205, National Aeronautics and Space Administration, NASA Lewis Research Center, June 1977.

[10]Scharfe, M., Koo, J., and Azarnia, G., "DSMC Implementation of Experimentally-Based Xe^+ + Xe Differential Cross Sections for Electric Propulsion Modeling," 27th International Symposium on Rarefied Gas Dynamics, Pacific Grove, CA, July 2010.

[11]Miller, J. S., Pullins, S. H., Levandier, D. J., Chiu, Y.-H., and Dressler, R. A., "Xenon Charge Exchange Cross Sections for Electrostatic Thruster Models," *Journal of Applied Physics*, Vol. 91, No. 3, February 2002, pp. 984–991.

[12]Brieda, L., *Development of the DRACO ES-PIC Code and Fully-Kinetic Simulation of Ion Beam Neutralization*, Master's thesis, Virginia Polytechnic Institute and State University, June 2005.

[13]Foster, J. E., Patterson, M. J., Pencil, E. J., McEwen, H. K., and Diaz, E. M., "Plasma Characteristics Measured in the Plume of a NEXT Multi-Thruster Array," AIAA Paper 2006-5181, *42nd AIAA/ASME/SAE/ASEE Joint Propulsion Conference & Exhibit*, Sacramento, CA, July 2006.

[14]Mandell, M. J., Davis, V. A., Pencil, E. J., and Patterson, M. J., "Modeling the NEXT Multithruster Array Test With NASCAP-2k," *IEEE Transactions on Plasma Science*, Vol. 36, No. 5, October 2008, pp. 2309–2318.

[15]Pencil, E. J., Foster, J. E., Patterson, M. J., Diaz, E. M., Van Noord, J. L., and McEwen, H. K., "Ion Beam Characterization of a NEXT Multi-Thruster Array Plume," AIAA Paper 2006-5182, *42nd AIAA/ASME/SAE/ASEE Joint Propulsion Conference & Exhibit*, Sacramento, CA, July 2006.